White Rose Research Online

eprints@whiterose.ac.uk
https://eprints.whiterose.ac.uk
Universities of Leeds, Sheffield and York

Deposited via The University of Sheffield.

White Rose Research Online URL for this paper:
https://eprints.whiterose.ac.uk/id/eprint/128206/

Version: Published Version

Article:
Romano-Acosta, L.F., Álvarez-Elcoro, I., Zapata-Hernandez, O. et al. (2018) Optimization of heating cycles prior forging for large steel ingots based on a simulation model. Materials Performance and Characterization, 7 (1). pp. 33-48.

https://doi.org/10.1520/MPC20170139

Reuse
Items deposited in White Rose Research Online are protected by copyright, with all rights reserved unless indicated otherwise. They may be downloaded and/or printed for private study, or other acts as permitted by national copyright laws. The publisher or other rights holders may allow further reproduction and re-use of the full text version. This is indicated by the licence information on the White Rose Research Online record for the item.

Takedown
If you consider content in White Rose Research Online to be in breach of UK law, please notify us by emailing eprints@whiterose.ac.uk including the URL of the record and the reason for the withdrawal request.

ASTM INTERNATIONAL

Materials Performance and Characterization

L. F. Romano-Acosta,[1] I. Álvarez-Elcoro,[2] O. Zapata-Hernandez,[2] and L. Leduc-Lezama[2]

DOI: 10.1520/MPC20170139

Optimization of Heating Cycles Prior Forging for Large Steel Ingots Based on a Simulation Model

VOL. 7 / NO. 1 / 2018

Materials Performance and Characterization

doi:10.1520/MPC20170139 / Vol. 7 / No. 1 / 2018 / available online at www.astm.org

L. F. Romano-Acosta,[1] I. Álvarez-Elcoro,[2] O. Zapata-Hernandez,[2] and L. Leduc-Lezama[2]

Optimization of Heating Cycles Prior Forging for Large Steel Ingots Based on a Simulation Model

Reference

Romano-Acosta, L. F., Álvarez-Elcoro, I., Zapata-Hernandez, O., and Leduc-Lezama, L., "Optimization of Heating Cycles Prior Forging for Large Steel Ingots Based on a Simulation Model," *Materials Performance and Characterization*, Vol. 7, No. 1, 2018, pp. 33–48, https://doi.org/10.1520/MPC20170139. ISSN 2379-1365

ABSTRACT

A simulation model has been used to calculate temperature distribution and internal stresses of steel ingots. The aim of this study is to optimize the heating cycles without compromising the mechanical integrity of the ingots, which ideally will result in a reduction in energy consumption and an increase in furnace productivity. The heating cycles of three ingots of different materials (ASTM A105, AISI 4330, and AISI 8630) and sizes (1.60, 1.75 and 1.32 m) are optimized. The optimization procedure of the heating cycle is based on a time reduction at each step of the set point. The phase transformation temperature at the ingot center was taken as a reference because this is where the higher stresses are developed. A sample of a 1 m ∅ AISI 8630 ingot was characterized with a Scanning Electron Microscope, Energy-dispersive X-ray Spectroscopy, X-Ray Diffraction, and Differential Scanning Calorimetry. Results show precipitates in the as-cast condition, which will eventually be dissolved after a complete heating cycle.

Keywords

steel ingot, thermal stresses, reheating, forging, simulation, characterization, cycle optimization, precipitates

Manuscript received August 30, 2017; accepted for publication November 7, 2017; published online February 14, 2018.

[1] Facultad de Ingeniería Mecánica y Eléctrica, Universidad Autónoma de Nuevo León, Pedro de Alba s/n, San Nicolás de los Garza, Nuevo León, C.P. 66450, México (Corresponding author), e-mail: luisfer1991@hotmail.com, https://orcid.org/0000-0002-0597-0706

[2] Facultad de Ingeniería Mecánica y Eléctrica, Universidad Autónoma de Nuevo León, Pedro de Alba s/n, San Nicolás de los Garza, Nuevo León, C.P. 66450, México

Copyright © 2018 by ASTM International, 100 Barr Harbor Drive, PO Box C700, West Conshohocken, PA 19428-2959

Introduction

At present, there is a high demand for production of large forged components for different industrial sectors such as oil and gas, aerospace, and some other applications. Before forging, ingot heating time is long, which generates huge furnace-operating costs and consumes a great amount of fuel. The energy used in the forging process is an important factor in the industrial economy, and heating costs represent a significant amount. The aim of the optimization procedure is to minimize heating costs, which are dependent on the ingot's total heating time. Optimum heating curves must be developed to reduce fuel consumption.

To ensure the quality of the final product, the production of large forging pieces is a process that requires a good knowledge of the thermal history of the piece. The efficacy of heating cycles can be assessed by three main features: the center of the ingot should reach the forging temperature, avoiding high-temperature gradients between the surface and the center during heating; the microstructure should be controlled and homogeneous; and the heating schedule should ensure that the thermal stresses are low enough to maintain the soundness of the material [1].

The heating rate, the microstructure, and the internal stresses of the ingot are the main effects to consider because they change in a complicated manner during heating. The temperature in an ingot could rise until it reaches the A_1 temperature and starts to transform into austenite. At that point, the latent heat effect changes the temperature distribution throughout the volume of the ingot, resulting in thermal and transformation stresses [2]. The purpose of the heating cycle is to achieve a homogeneous temperature distribution throughout the ingot while removing precipitates, mainly carbides, before the end of the cycle [3]. The ideal heating condition is when the ingot center and the surface temperatures are equal to the forging temperature, resulting in the dissolution of all carbides, and the maximum calculated thermal stress should be smaller than the fracture stress. This can be achieved, deforming shortly after the solidification, when the ingot is still at a high temperature; nevertheless, in this case this practice is not used because of the capacity of the plant. Therefore, it is necessary to calculate the time when the temperature difference between the ingot center and its surface is adequate for the forging operation. Time and heating rates are the two most important factors when defining the heating cycle, and they depend on the chemical composition, shape, and size of the ingot [4].

The finite element analysis method is frequently used to predict how a real object will react to forces, heat, flow of fluids, etc. Finite element analysis provides wider opportunities for numerical research in forging processes than some other methods [5]. The optimum heating time for forging is calculated using simulation models [6]. Because it is not necessary to carry out industrial tests with real material, it is profitable to design large ingot heating cycles using computer models because of the cost and time savings [7].

This work analyzes the possibility of optimizing the heating cycles for large steel ingots prior to forging. The ingots must meet the following three conditions: they must be without high temperature gradients when they reach the forging temperature, the structure must be as homogeneous as possible, and the thermal stresses must be smaller than the fracture stresses. To achieve this, a study of the heat transfer in the furnace was performed. Industrial tests were carried out with thermocouples in the ingots to obtain the heat transfer coefficient value from the result of the recorded temperature. These temperature measurements were used to create a simulation model that could predict

the temperature distribution and the stress levels inside the ingot during heating. In addition, dissolution of precipitates was studied to determine the soaking time needed to homogenize the ingot, i.e., minimize segregation, and ensure that all parts of the ingot were the same temperature. The total time of the heating cycle is always related to ingot size.

Methods

Three different specifications of cylindrical tapered ingots were analyzed: a 63-in. ∅ based on ASTM A105, *Standard Specification for Carbon Steel Forgings for Piping Applications* [8], i.e., Ingot A; a 69-in. ∅ made with AISI 4330, i.e., Ingot B; and a 52-in. ∅ made with AISI 8630, i.e., Ingot C, with estimated weights of 32.6, 35.4, and 17.3 tons, respectively. For the as-cast condition, an AISI 8630 sample of a 39-in.-diameter ingot was used.

Temperature measurements during heating were taken to compare with the computer model measurements; several holes that measured $\frac{3}{16}$ in. in diameter were made over the ingot hot top with different depths in which to place ⅛ in. ∅ K-type thermocouples. Once the thermocouples were in place, the holes were covered with ceramic fiber, which acted as thermal insulation. Ingot A had one hole that was 16 in. deep, Ingot B had one hole that was 9 in. deep, both of which were at the center of the hot top, and Ingot C had one hole that was 14 in. deep at the center of the hot top and another hole that was 13 in. deep at mid radio. The temperature was monitored during heating with a Graphical and Chart Data Recorder. For these tests, a car bottom furnace with a front door was used. It was equipped with high-speed burners, consumed natural gas as fuel, had automatic/manual controls, and the maximum temperature it could reach was 1,350°C. The furnace had a capacity of 100 tons and had heat exchangers wherein the air was preheated to a temperature between 200°C and 300°C. A ratio of 10 to 1 in the air-gas supply was used for greater efficiency in the burners. The furnace had eight burners (four on each side) that were located at the top of the side walls where the thermocouples were also found to monitor the temperature inside the oven. The floors of the ovens were made of refractory concrete to support the loads, and the walls were insulated with ceramic fiber.

MATERIAL CHARACTERIZATION

One of the requirements for forging an ingot that comes from a casting process is to ensure the ingot's structure is as homogeneous as possible; to achieve this, it is necessary to provide energy in the form of heat to dissolve all kinds of precipitates, which are mainly carbides, in the matrix that are generated during the solidification process. Scanning Electron Microscopy (SEM), X-Ray Diffraction (XRD), and Differential Scanning Calorimetry (DSC) analyses were performed to determine whether inclusions were present.

SEM was used to find different phases and to determine the size and morphology of these phases. A 39-in. diameter AISI 8630 ingot specimen was scanned in as-cast condition and then imaged at different magnifications with Backscattered Electron, Secondary Electron, and Energy-dispersive X-ray spectroscopy; this specimen was also analyzed by XRD and DSC.

For the XRD analysis, a D8 Advance diffractometer (Bruker, Billerica, MA) equipped with a copper source was used. The diffractometer was operated with a voltage of 40 kV and a current of 30 mA. The data were collected in a range of 2 θ from 20° to 100° at every 0.02° with an analysis time of 30 minutes per specimen. The specimen was kept rotating at

FIG. 1

Sketch drawn for Ingot A [9].

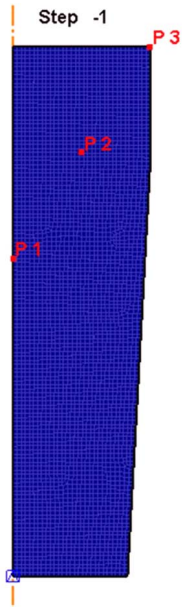

a speed of 15 r/min to minimize the effects of preferential orientation and to favor the random orientation of the crystals. A qualitative analysis was made by identifying the pattern of each phase using DIFFRAC.SUITE EVA software (Bruker, Billerica, MA).

A DSC 404 F3 Pegasus (Netzsch Group, Selb, Germany) was used for the phase transformation kinetics and the analysis of the dissolution of precipitates. Alumina crucibles with 99.6 % purity were selected. The crucible used to place the specimens had a mass of 297.9 mg, and the crucible for reference weighed 316.9 mg. Five specimens were heated up to 1,200°C at a rate of 10, 15, 20, 35, and 50°K/min, respectively. To carry out these tests, the DSC furnace was purged to vacuum up to 94 %; argon was introduced as an inert atmosphere. In order to avoid unexpected results, smoothing their surfaces and minimizing the stresses left by mechanical strain, the specimens were electropolished at 10 V for 10 seconds; the electrolyte used in the electropolishing contained 800 mL of ethanol, 140 mL of distilled water, and 60 mL of perchloric acid 60 % (HClO4).

SIMULATION MODEL

The prediction of temperatures during heating is a very important process because it allows us to know how much time is needed to obtain the conditions required in the ingot that is to be deformed. The heating was simulated by the finite element method using the DEFORM software (Scientific Formatting Technologies Corporation, Columbus, OH), in which the ingot geometries were sketched and the thermal properties of each material were calculated using the JMatPro software (Sente Software Ltd., Guildford, England, UK). The material properties used for this analysis are as follows: thermal conductivity, heat capacity, density, Young's modulus, thermal expansion coefficient, Poisson's ratio, flow stress curves, latent heat due to phase transformation, emissivity, and the heat transfer coefficient. The simulation model created was a two-dimensional elastoplastic model with a symmetry plane in the center of the ingot to reduce computational time. Fig. 1 shows

TABLE 1
Heat transfer coefficient and emissivity values used for the simulation model.

Temperature (°C)	Emissivity	Heat Transfer Coefficient, h, $\left(\frac{N}{s \cdot mm \cdot °C}\right)$
25–700	0.5	0.015
701–1,280	0.8	

a sketch of Ingot A, where the coolest and hottest points can be identified as P1 and P3, respectively. An element between these two points, P2, was also analyzed and is considered the middle radius. The porosity that could be present for the as-cast condition was not considered. The model considers the ingot to have a circular profile and a conical volume with a smooth surface; in addition, the ingot is considered to have no residual stresses at the beginning of the heating process. The simulation model for the industrial furnace used in this analysis was based on the heating test of Ingot A. Trial and error adjustments were made to the model to estimate the coefficient of heat transfer inside the furnace. This model considers convection and radiation for heat transfer at the ingots surface, and only thermal conduction is considered at the ingot center [9].

The values of the heat transfer coefficient (h) and emissivity that gave the best result are presented in **Table 1**. The emissivity was taken in two temperature ranges because of the oxidation of the ingot surface and the difference in the phases that exist in these temperature ranges.

Once the correct simulation base model is generated, the temperature at any point in the ingot, at any grade and steel profile, can be predicted. The heating curves of the industrial tests were modified in the model and were designed with a shorter total heating time. These curves not only guarantee that the calculated temperature will reach the temperature required for forging but also that the stress values during heating will not exceed the stresses calculated in the industrial curves.

The thermal stresses are generated by the expansion or contraction of the material caused by the thermal deformation and phase transformations. The thermal stress (σ) is related to the thermal expansion coefficient (α), the Young's modulus (E), and the temperature difference between two points (ΔT) (Eq 1) [10].

$$\sigma = E\alpha\Delta T \tag{1}$$

Results

COMPARISON BETWEEN CALCULATED AND MEASURED TEMPERATURES

Fig. 2 shows the original heating cycle for Ingot A; the stepwise curve is the programmed temperature increase of the furnace for that ingot. The measured temperature at the center of the ingot is also plotted in the graph in this figure, together with the calculated values with the model. Additionally, the two horizontal lines represent the temperature range (A_1 and A_3) where the ferrite-austenite phase transformation takes place.

For Ingot B, the same graphs as those for Ingot A are plotted in **Fig. 3**; in this case, the furnace temperature does not match the programmed setup curve because at the beginning of the cycle the furnace was preheated before the heating cycle started. After the setup

FIG. 2

Comparison of experimental and simulation results for Ingot A [9].

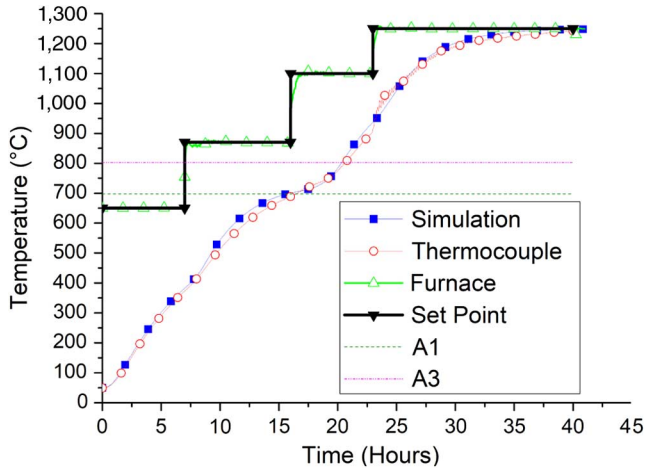

FIG. 3

Comparison of experimental and simulation results for Ingot B [9].

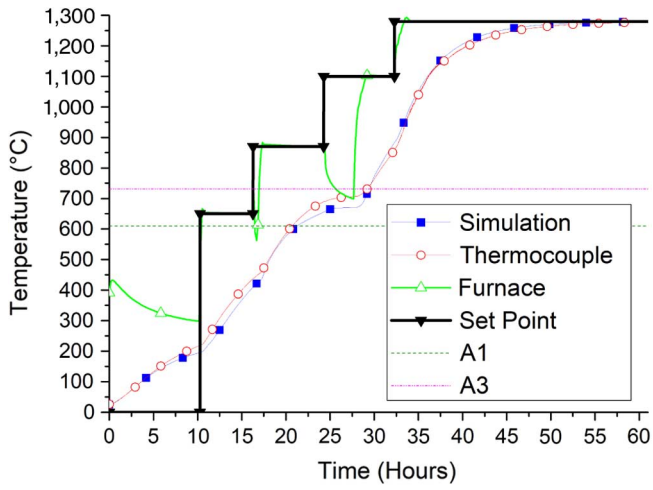

curve starts, the furnace temperature follows it. The furnace temperature deviated from the setup curve because of a temporary burner shutdown, which was fixed in a relatively short time; after that, the furnace followed the setup curve. Here again, the temperature of the ingot surface followed the temperature of the furnace, and the measured temperature at the center is shown together with the calculated temperature.

In Fig. 4a and 4b, the same curves are plotted for Ingot C, one for the temperature at the center of the ingot and another for the temperature at the middle radius. The description, as in the other cases, also applies here, and there is a small discrepancy of the measured temperatures after the phase transformation wherein the temperature of the center is slightly higher than the middle radius and is probably due to a change in position of one of the thermocouples. However, at the end of the cycle the temperatures converge to the

FIG. 4 Comparison of experimental and simulation results for Ingot C: (a) for the measured and calculated temperature at the ingot center and (b) for the measured and calculated temperature at the middle radius.

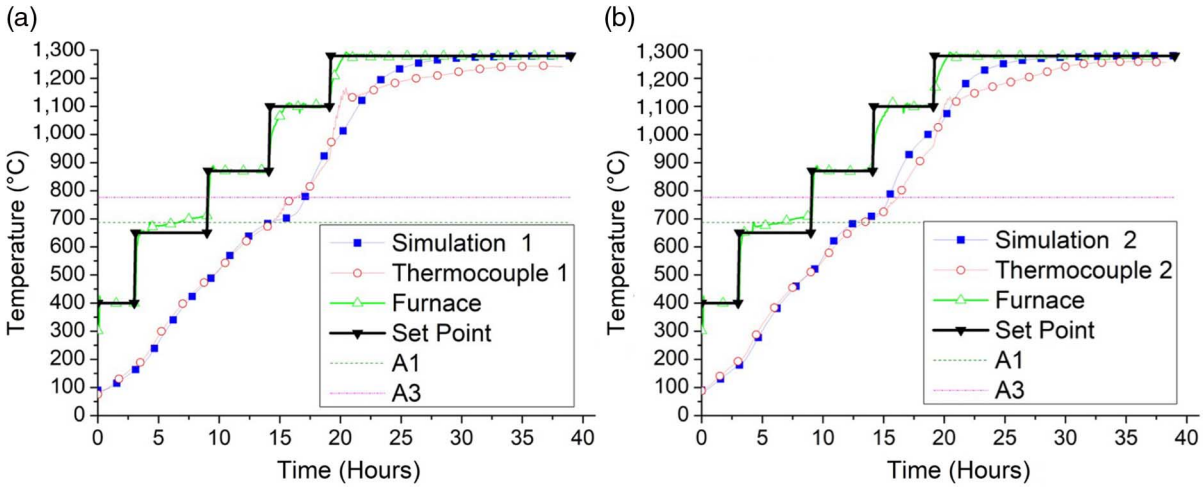

target temperature. It is clear that there is agreement between the measured and calculated temperatures.

THERMAL AND TRANSFORMATION STRESSES

The maximum principal stress (σ_1) is used to see if a specific part of the ingot is in a state of compression or tension. Maximum principal and hydrostatic stresses are important in determining whether the ingot will crack during heating. These stresses will vary, depending on the heating rate and the phase transformation kinetics.

In the present study, the σ_1 generated in the original heating cycles were taken as a reference because it is known that with these cycles the ingots did not present any damage or problems in forging.

The σ_1 was calculated for the center, middle radius, and surface for each ingot. The results are shown in Fig. 5.

Although there are stages during the heating cycle in which the σ_1 in the middle radius of the ingot is greater than the stress at the center, these stresses are always lower than the highest stress in the center at the end of the phase transformation.

The optimized curves were designed so that the σ_1 would not exceed the stresses calculated in the ingot center of the original cycles. Because of this, the ingots are not expected to have problems when forged according to the optimized heating curves.

INGOT HOMOGENIZATION

Fig. 6 shows a SEM image of the AISI 8630 specimen from the ingot center that was obtained by backscattered electrons. Here, a chromium carbide can be seen with a brighter tone than the matrix that is 3 μm in length. According to the JMatPro, this kind of carbide in the AISI 8630 steel grade starts to dissolve at 750°C. In all heating cycles considered, the furnace was kept above this temperature for more than 10 hours, which is enough time to guarantee the dissolution of all carbides.

FIG. 5 The σ_1 in the center, middle radius, and surface of Ingots A, B, and C.

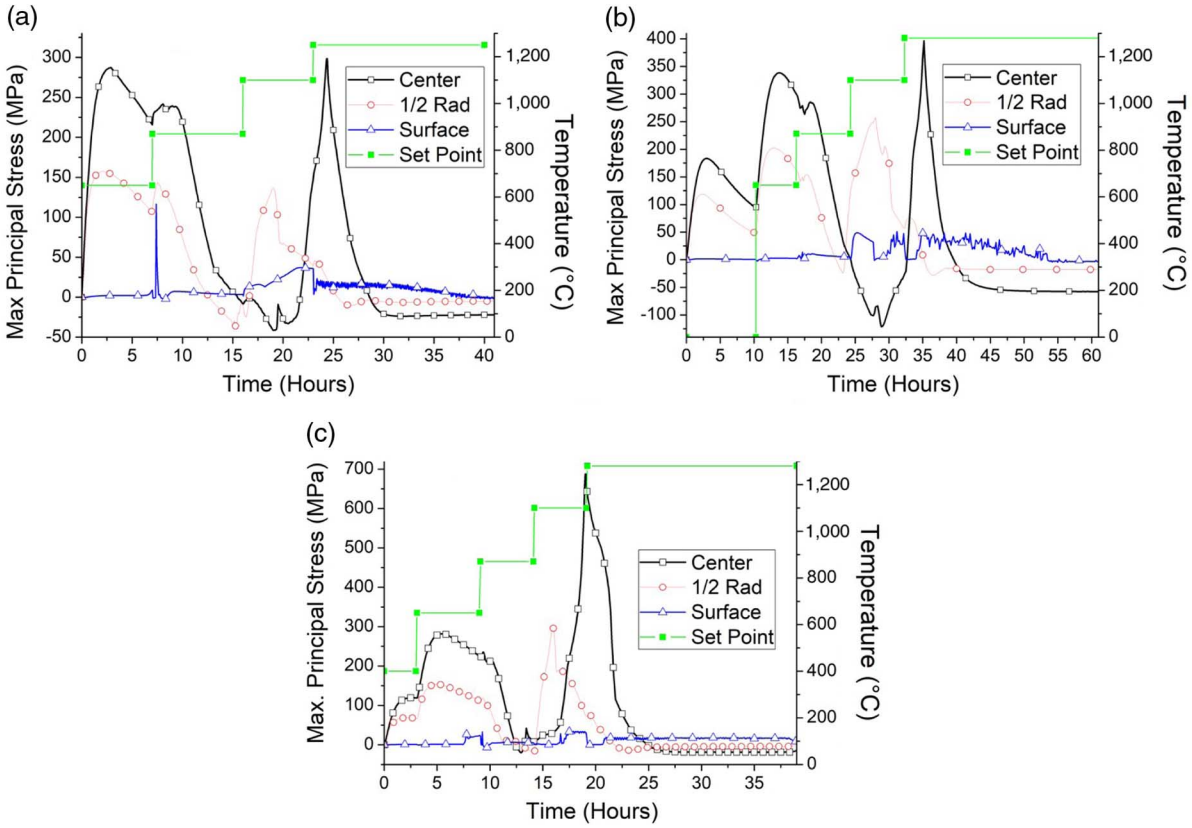

FIG. 6 Image of the AISI 8630 ingot center at room temperature that was generated by a backscattered electron detector. The points marked (a) and (b) were analyzed to show the chemical composition and the diffraction pattern (XRD).

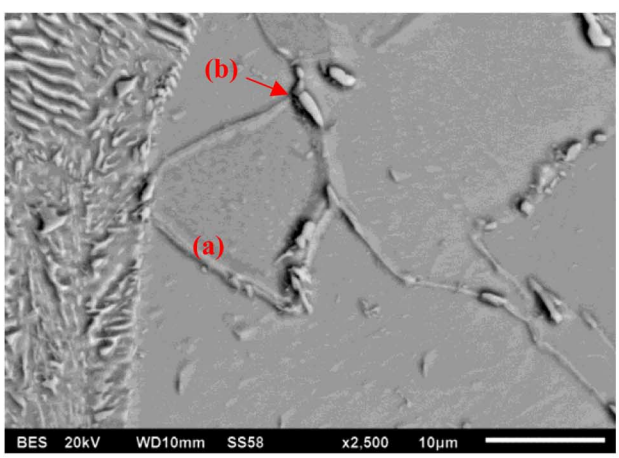

(a)

Element	Wt %	At %
CK	04.38	17.64
MoL	01.28	00.65
CrK	01.20	01.12
MnK	01.66	01.46
FeK	89.48	77.49
NiK	02.00	01.65
Matrix	Correction	ZAF

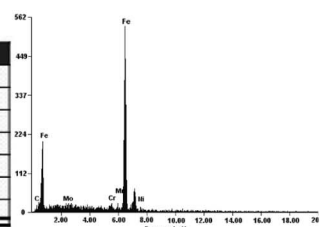

(b)

Element	Wt %	At %
CK	09.96	34.00
MoL	01.57	00.67
CrK	06.32	04.98
MnK	03.69	02.76
FeK	77.34	56.80
NiK	01.12	00.78
Matrix	Correction	ZAF

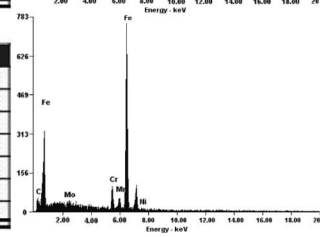

FIG. 7 XRD patterns of the AISI 8630 ingot center.

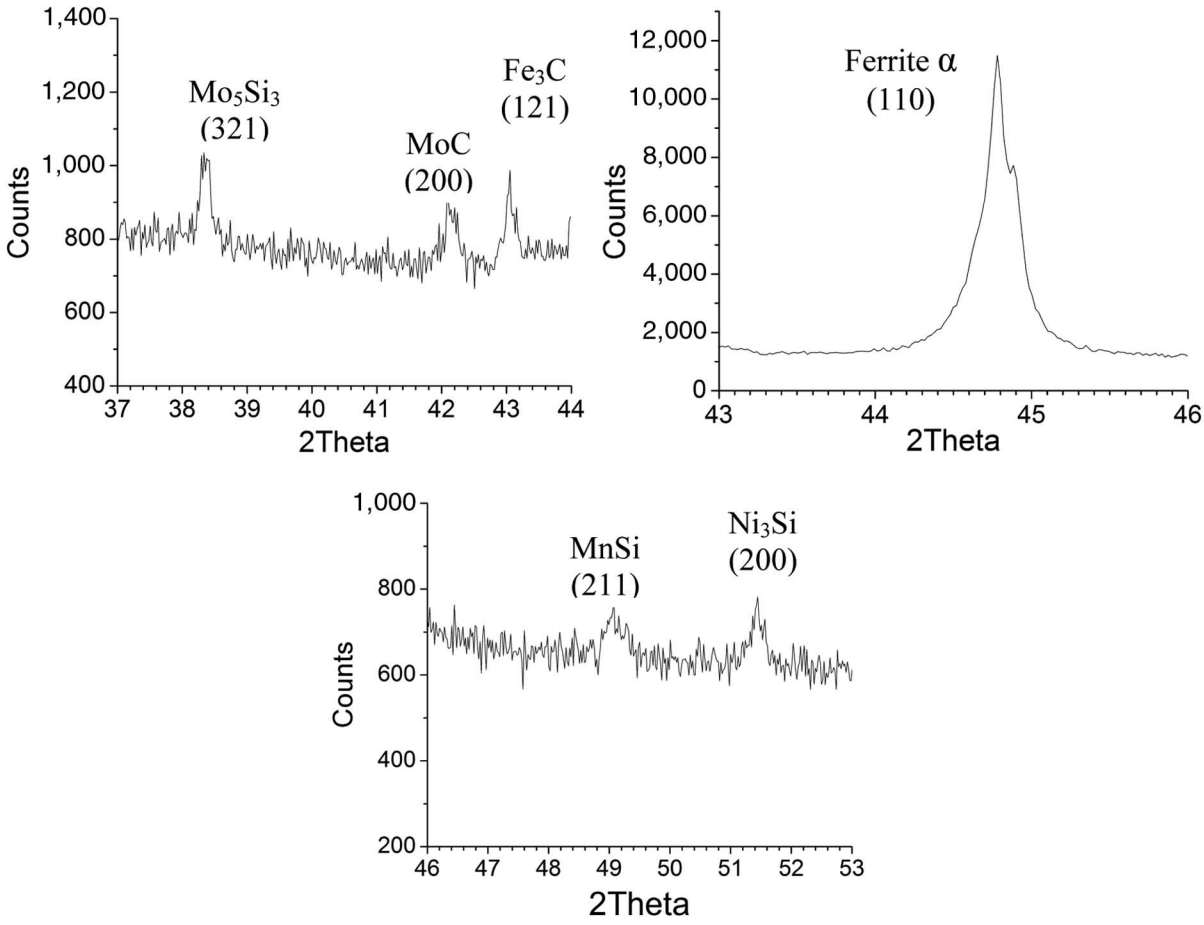

Fig. 7 shows the presence of all precipitates predicted by JMatPro in an XRD pattern. Additionally, other phases, such as molybdenum carbide and manganese silicide, were identified at room temperature. It is thought that the presence of these phases is due to microsegregation. Nevertheless, JMatPro and Epp et al. [11] indicate that these compounds dissolve at temperatures below that of the last step of the set point in the heating cycle.

Fig. 8 shows that all specimens evaluated have endothermic peaks at 788°C, which indicates the phase transformation from ferrite to austenite; this temperature is similar to that indicated by JMatPro. At 760°C, there is another peak that is attributed to the dissolution of pearlite in austenite and to the dissolution temperature of carbides of the type $M_{23}C_6$, which is 750°C, where M represents iron, molybdenum, or chromium, which also coincides with JMatPro. The curves in **Fig. 8** also show an exothermic process at 470°C of very low energy attributed to M_7C_3-type carbide, which is dissolved at this temperature. Even though, according to JMatPro, the M_7C_3-type carbide should not be present in the AISI 8630 steel grade, the carbide is in the specimen heated in the DSC in accordance with XRD analysis because of microsegregation. In the specimens heated at 20, 35, and 50°K/min, an exothermic reaction is observed with very low energy at around 1,050°C. It is

FIG. 8

Effect of heating rate on the energy change in DSC.

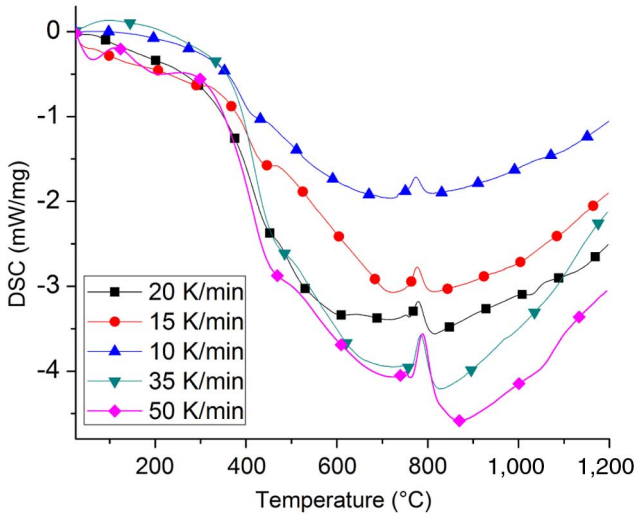

FIG. 9

Comparison between original and optimized heating cycle for Ingot A.

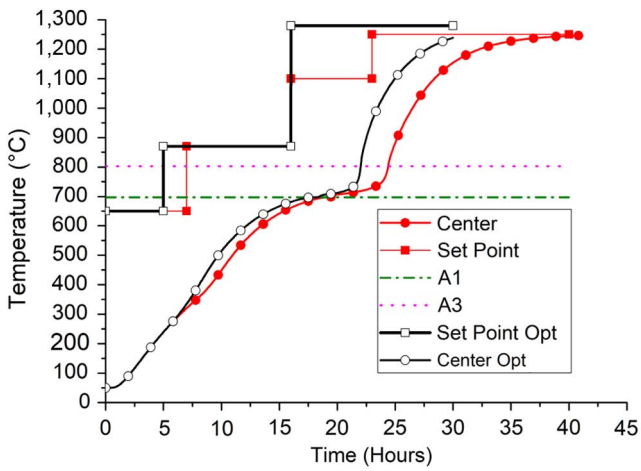

thought to be the dissolution of an MC-type carbide, which may contain niobium or titanium-vanadium since its dissolution temperature is in that range [12].

HEATING OPTIMIZATION

Heating curves are designed in several steps that include increasing the temperature and producing temperature gradients between the center and surface at each step. The largest temperature gradient during the complete heating curve happens at the center when the last increment in the setup corresponds with the end of the phase transformation. Fig. 10 shows the evolution of the σ_1 in Ingot A, and a similar behavior was observed for the hydrostatic stress. In this case, the maximum value for σ_1 is 300 MPa.

FIG. 10

σ_1 in the original and optimized heating cycle for Ingot A.

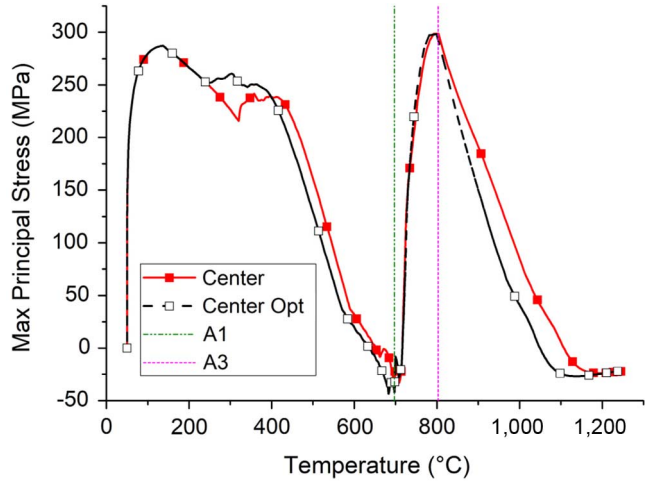

An optimized cycle was designed for Ingot A, reducing the original heating time by 26 % and ensuring that σ_1 does not exceed the value of the original cycle and that the center reaches the forging temperature, as shown in Fig. 9 and Fig. 10, respectively. Time and temperature reached by the ingot meet the condition that there should not be undissolved carbides. The σ_1 generated in the original cycle was taken as a reference for optimization.

The heating cycle for Ingot B, as shown in Fig. 11, was redesigned, which reduced the total time of the original cycle by 27 % , ensuring that the σ_1 set by the ingot center was not exceeded; the highest σ_1 in Ingot B is 396 MPa. This occurs at the center of the ingot after 35 hours and is when the maximum temperature gradient is reached, as seen in Fig. 12, which is just about the time the center reaches the A_3 temperature. Even though, at the beginning of the optimized cycle, the σ_1 is greater than that of the original cycle, this stress is lower than the stress registered at the end of the center transformation at a higher temperature.

FIG. 11

Comparison between the original and optimized heating cycles for Ingot B.

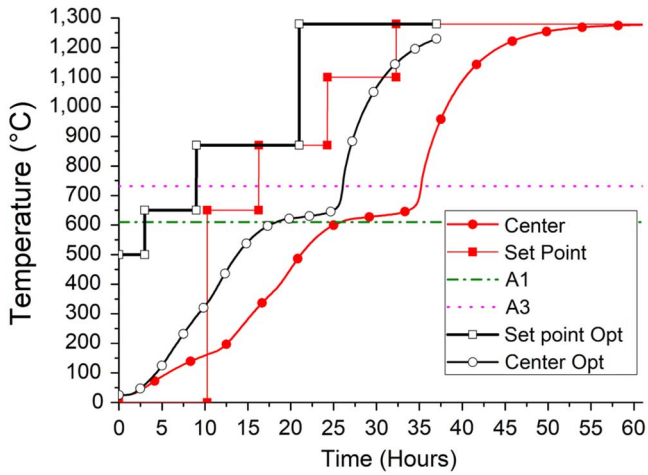

FIG. 12

The σ_1 in the original and optimized heating cycles for Ingot B.

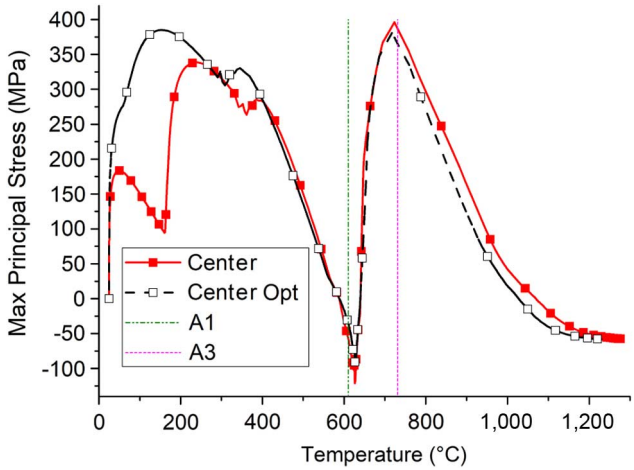

FIG. 13

Comparison between the original and optimized heating cycles for Ingot C.

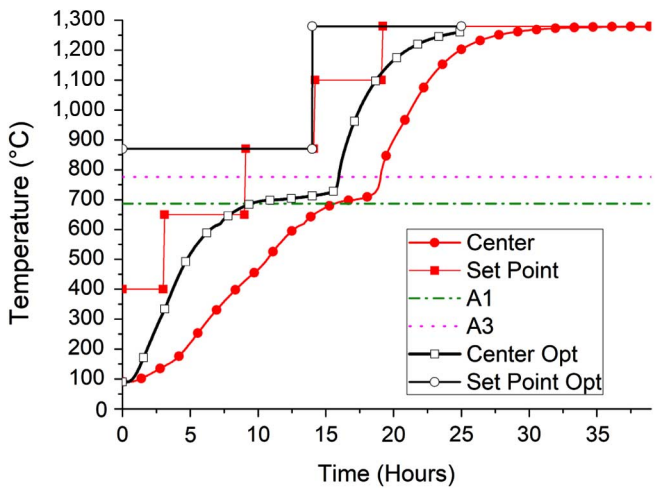

The heating cycle optimized for Ingot C reduced the original cycle by 25 %, as shown in Fig. 13. Since the diameter of this ingot is the smallest of the three ingots studied, it is possible to start directly at the 870°C step, as the temperature gradient generated at the beginning of the cycle does not cause stress that exceeds the stress limit established by the center of the ingot at the end of its transformation, as shown in Fig. 14. The center and surface are closer to each other in this case, and the temperature gradient is smaller than that of the other two ingots.

Discussion

The σ_1 is reached at the end of the transformation of the ingot center. From the beginning of the heating cycle until the point before the center reaches the transformation

FIG. 14

The σ_1 in the original and optimized heating cycles for Ingot C.

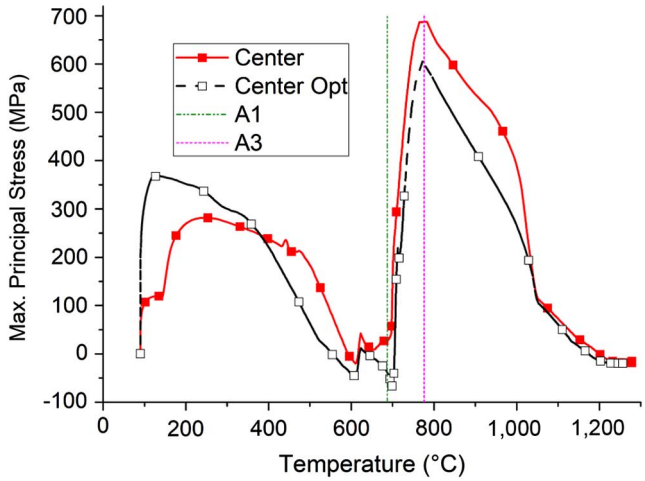

temperature, the behavior of the σ_1 is governed by the temperature difference between the center and the surface, while from the time the ingot center begins its transformation to austenite until the end of the cycle, the σ_1 is governed by the phase transformation; during the transformation from ferrite to austenite, the material undergoes a volume contraction while a point nearer the surface is expands in the austenite phase. For this reason, when the center of the ingot ends its transformation, the σ_1 decreases as it begins to expand in the austenite phase, having the same direction of deformation as the rest of the ingot. During the final stage of the heating cycle, the center of the ingot is exposed to compression.

The critical moment while reheating an ingot is when the center finishes its transition to austenite. The temperature at the center lags because of the latent heat used for the transformation, while the surface continues to increase its temperature, which creates the largest temperature gradient. In Fig. 10, σ_1 at the ingot center is plotted as a function of time; after the ingot center finishes its transformation, the stress decreases because the center increases in temperature, and the surface has a constant temperature, which decreases the temperature difference and hence the stress itself. Stresses are reduced when the temperature of the ingot surface does not increase while the transformation is taking place but the core continues to increase in temperature. This trend continues until the center begins its transformation. In all three cases, the setup curve increases in temperature when the center is about to cross the A_3 temperature. This fact increases the temperature gradient to the maximum value, hence the internal stresses are produced. All of this agrees with Alam, Goetz, and Semiatin [13], who suggest that the failure is controlled by a criterion of maximum normal stress, and the ingots that failed presented cracks initially in the center of the ingot and then propagated to the lateral surfaces. The failure is caused by axial stresses.

The optimization process of the heating curves is based on the reduction of time in each step of the set point. The phase transformation in the center of the ingot was taken as a strategic point because it is where the highest stress is presented during the heating cycle.

The step at 870°C was considered the most important step in maintaining stresses in a safe range because it is located above the A_3 temperature; this step should be long enough

for the center to begin its transformation to austenite (which means that the other points nearer the surface of the ingot should have already finished their transformations or are in the process of doing so). This step was longer in the three cases for each optimized cycle. Although it differs in the goal of heating time reduction, the stresses should be kept at an acceptable level. The heating time can be reduced in other stages of the cycle or a step could also be eliminated.

The last step in the set point, when the temperature is at 1,280°C, is in charge of finishing the ingot's transformation. The principal stresses fall through this stage of the heating cycle because the temperature gradient is becoming smaller, and the remaining time at this temperature needs to be used to bring the center of the ingot to forging temperature.

The step at 1,100°C was no longer needed in any of the optimized cycles because the center of the ingot had already started transforming during the step at 870°C. This means that the phase transformation through the radial length of the ingot is slower and, consequently, the stresses do not exceed the settled limit. The temperature gradient between the center and surface generated by the elimination of this step did not cause a problem in the behavior of the stresses.

Because of the diameter size of Ingot C, it is possible to eliminate the step at 650°C. For this test, the curve was designed to start directly with the step at 870°C because the temperature gradient at the beginning of the cycle did not cause the stresses to exceed the limit set by the center of the ingot at the end of its phase transformation.

The strength of the steel decreases with an increase in temperature. The stress value during the first stage of the optimized heating cycle "A" is greater than the stress value in the first stage of the original heating cycle, but it is still less than the maximum stress in the center of the ingot at the end of its transformation.

According to the simulation model, there is slightly greater but imperceptible plastic deformation in the optimized cycle than in the original cycles.

The simulation model shows that the temperature of the surface rises more rapidly than the temperature in the center of the ingot at the beginning of the heating cycle. The latent heat effect is not observed at the surface because it is exposed to both convection and radiation from the flame and the walls of the furnace. Since radiation is the main mechanism of heat transfer, the temperature at the surface increased quickly at transformation temperature because of the increase in emissivity at that temperature that is produced by the oxidation of the ingot surface [14].

Based on the calculations of the optimized heating cycles, it can be concluded that the σ_1 are maintained in an acceptable range when the temperature on the ingot surface or the set point is at a temperature just above A_3 and the center has begun its phase transformation. This is due to the fact that, through the ingot profile, i.e., from the surface to the center of the ingot, the phase transformation kinetics are slower because it is at a lower temperature than in the original heating cycle and, consequently, the volume change caused by phase transformation would be slower.

A ratio of the time required in the last step of the heating curve, that is at 1,280°C, was generated (Eq 2) so that the center of the ingot could reach the forging temperature, depending on the diameter of the ingot. This ratio is shown in the following equation:

$$\frac{th_{om}}{Dp} \cong 0.22 \tag{2}$$

Where th_{om} is the time needed, in hours, to thermally homogenize between the center and the surface of the ingot. *Dp* is the diameter of the ingot profile in inches.

Conclusions

Industrial tests were performed to measure ingot temperature as a function of heating time at the center of the ingot to compare with calculated values for three different steel grades and sizes. The temperature and stress distributions within the ingot were calculated from the ingot properties and the setup curve as a function of time.

The temperature required for forging is achieved in the three tests, both the calculated temperature in the center and actual measurements, which is one of the main objectives of reheating. Both original and optimized heating cycles, times, and heating temperatures are sufficient to dissolve different precipitates found in the center of the ingot. The size of the piece to be treated can influence the soaking time but not the temperature.

Simulation models for large forgings are useful to understand the thermal, mechanical, and metallurgical phenomena that occur during the heating process. This simulation model allows for the analysis of the optimization of the heating curves, maintenance of the quality of the ingot, preservation of operation time and energy, and also an increase in the productivity of the furnaces. The simulation model results agree with the three plant measurements, and this reliable model was used to predict what would happen with the optimized heating curves.

Thermal stresses in optimized heating cycles do not exceed the maximum stress of the original cycles. Internal stresses produced during the original heating cycles were not high enough to crack the ingots, and, by the same token, it is expected that optimized heating cycles are not either.

σ_1 are maintained in an acceptable range when the surface temperature of the ingot (set point) is at a temperature above A_3 until the center starts its phase transformation; and, from the surface toward the center of the ingot, transformation kinetics are slower because they are at a lower temperature (870°C) than in the original heating cycle; therefore, the volume change by transformation will be slower.

ACKNOWLEDGMENTS

The authors want to acknowledge FRISA and CONACYT for their support in carrying out this project.

References

[1] Chandrasekharan, S., 1992, "Optimization of Preheating Schedules for Nickel Base Superalloy Ingots Using Finite Element Analysis," M.S. thesis, Ohio State University, Columbus, OH.

[2] Inoue, T., Nagaki, S., Kishino, T., and Monkawa, M., "Description of Transformation Kinetics, Heat Conduction and Elastic-Plastic Stress in the Course of Quenching and Tempering of Some Steels," *Ing. Archiv.*, Vol. 50, No. 5, 1981, pp. 315–327, https://doi.org/10.1007/BF00778427

[3] Fantini, G., Fioletti, F., Formentelli, M., Guarneri, M., Gruttadauria, A., Mapelli, C., and Mombelli, D., "Study about Chemical Homogenization of Ingots and Optimization of Heating Cycle," *Metall. Ital.*, No. 3, 2013, pp. 47–52.

[4] Sun, R. C., "Determination of the Forging-Heating Schedule or a Large "HASTELLOY" Alloy X Ingot," *Metall. Trans.*, Vol. 1, No. 7, 1970, pp. 1881–1887, https://doi.org/10.1007/BF02642787
[5] Tomov, B. I., Gagov, V. I., and Radev, R. H., "Numerical Simulations of Hot Die Forging Processes Using Finite Element Method," *J. Mater. Process. Technol.*, Vols. 153–154, 2004, pp. 352–358, https://doi.org/10.1016/j.jmatprotec.2004.04.051
[6] Choi, S. K., Chun, M. S., Van Tyne, C. J., and Moon, Y. H., "Optimization of Open Die Forging of Round Shapes Using FEM Analysis," *J. Mater. Process. Technol.*, Vol. 172, No. 1, 2006, pp. 88–95, https://doi.org/10.1016/j.jmatprotec.2005.09.010
[7] Brada, G. A. and Van Tyne, C. J., "Modeling of Heating and Heat Treating Cycles for Large Forgings," *Ind. Heat.*, Vol. 63, 1996, pp. 6–11.
[8] ASTM A105, *Standard Specification for Carbon Steel Forgings for Piping Applications*, ASTM International, West Conshohocken, PA, 2014, www.astm.org
[9] Romano Acosta, L. F., Zapata, O., Álvarez, I., Cerda, R., and Lezama, L. L., "Simulation of Heating Cycles for Large Steel Ingots," *MRS Proc.*, Vol. 1812, 2016, pp. 23–28.
[10] Dieter, G. E., *Mechanical Metallurgy*, McGraw-Hill, New York, NY, 1961, p. 430.
[11] Epp, J., Surm, H., Kessler, O., and Hirsch, T., "In Situ X-Ray Phase Analysis and Computer Simulation of Carbide Dissolution of Ball Bearing Steel at Different Austenitizing Temperatures," *Acta Mater.*, Vol. 55, No. 17, 2007, pp. 5959–5967, https://doi.org/10.1016/j.actamat.2007.07.022
[12] Gong, P., Palmiere, E. J., and Rainforth, W. M., "Dissolution and Precipitation Behaviour in Steels Microalloyed with Niobium during Thermomechanical Processing," *Acta Mater.*, Vol. 97, 2015, pp. 392–403, https://doi.org/10.1016/j.actamat.2015.06.057
[13] Alam, M. K., Goetz, R. L., and Semiatin, S. L., "Modeling of Thermal Stresses and Thermal Cracking during Heating of Large Ingots," *J. Manuf. Sci. Eng.*, Vol. 118, No. 2, 1996, pp. 235–243, https://doi.org/10.1115/1.2831016
[14] Shi, D., Pan, Y., Zhu, Z., and Sun, J., "Effect on the Spectral Emissivity of SPHC Steel by Surface Oxidization," *Int. J. Thermophys.*, Vol. 34, No. 6, 2013, pp. 1100–1109, https://doi.org/10.1007/s10765-013-1476-1